

Membrane Biofouling

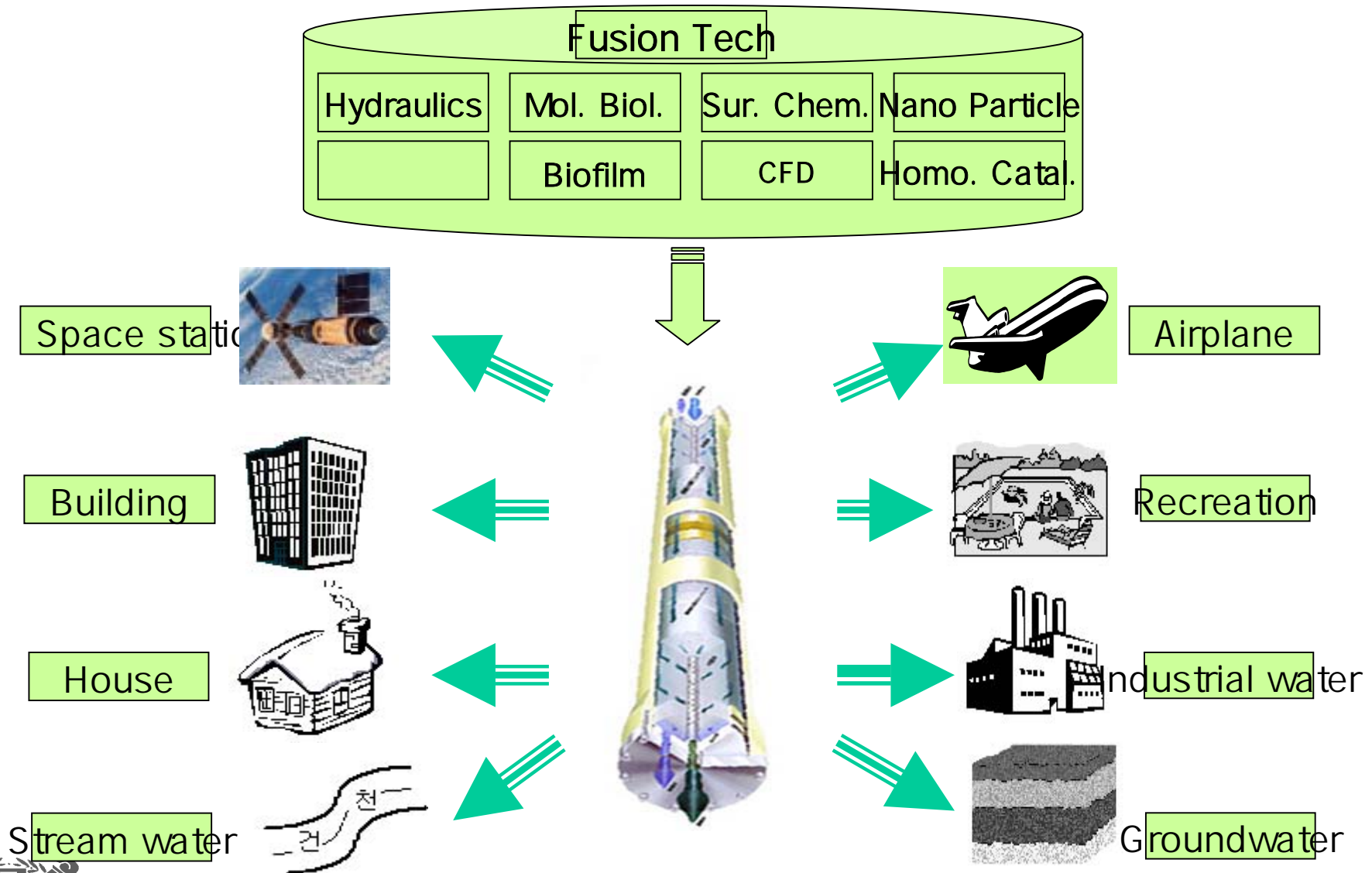
Director and Prof. Chung-Hak LEE,

**Institute of Environment Protection and Safety
Water Environment – Membrane Technology Lab.
School of Chemical Engineering,**

Seoul National University, KOREA



Application of Membrane Processes in Water Environment



MBR : Worldwide Buisness

~ thousands of installations of MBRs in the World

Vivendi (France), Memcore (USA)
Zenon (Canada),
Mitsubishi, Kuboda (Japan), etc..

~ 750 MBRs in Korea since last 6 years



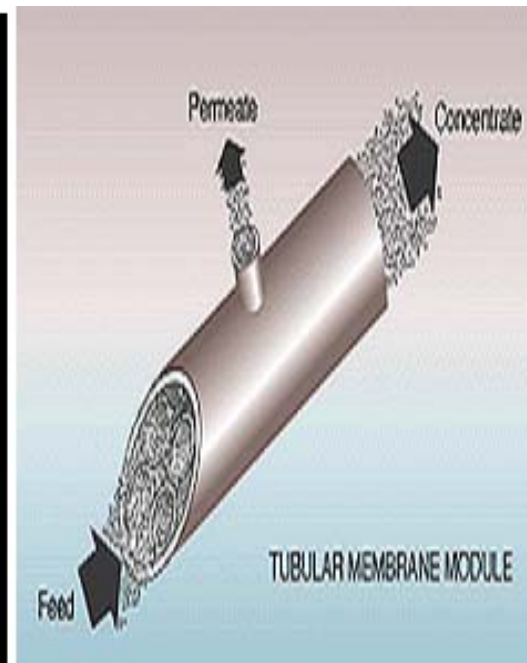
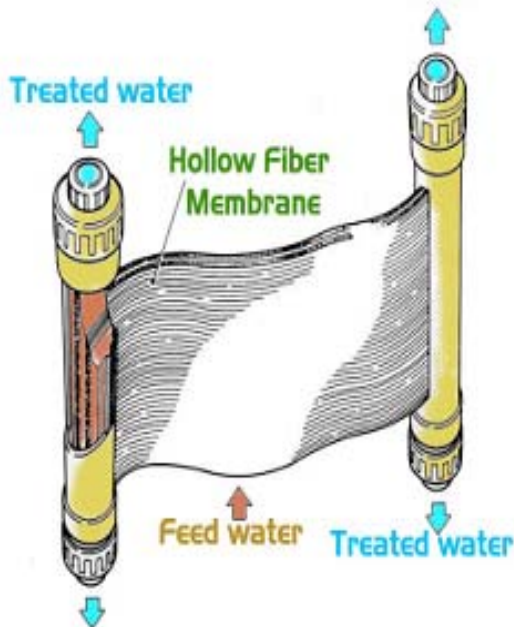
Commercial MBR plants in Korea *2003(2002)

Membrane Manufacturer	Module type	Company	Trade mark	Membrane Material (PORE SIZE, μm)	Starting Year	Number of Installation	Highest capacity (M^3/d)	Filtration Mode
MRC (JAPAN)	HOLLOW FIBER MEMBRANE	KEC & HEC	SMAS & HANT	PE (0.4)	1997	403(300)	4,000(1,400)	DEAD-END FILTRATION
ZENON (CANADA)		SAE-HAN	ZENOGEM	PVDF (0.035)	2000	10(7)	1,000(300)	
KMS (KOREA)		KMS	-	PE (0.4)	2002	150(100)	600(225)	
SKC, E.N.E. (KOREA)		KOLON	KIMAS	PSF (0.1)	1998	10(10)	-	
天津膜天社 (CHINA)		RAPAH TECH	-	PVDF (0.1-0.4)	2002	10	-	
YUASA (JAPAN)	PLATE MEMBRANE	ZENIX ENG & JIN WOO ENV.	NIX-MBR	Polyolefin (0.4)	1999	68(67)	4,000(900)	
PURE ENVI-TECH (KOREA)		PURE ENVI-TECH	-	CPVC (0.25)	2002	20(2)	350(250)	
MEMBRATEK (SOUTH AFRICA)	TUBULAR MEMBRANE	AQUATECH	BIOSUF	PES (40,000Da)	1995	50(50)	2,000(2,000)	CROSSFLOW FILTRATION
RUSSIA		ZENIX ENG.	-	PSF (30,000Da)	1996	13(13)	200(-)	
						734(559)		

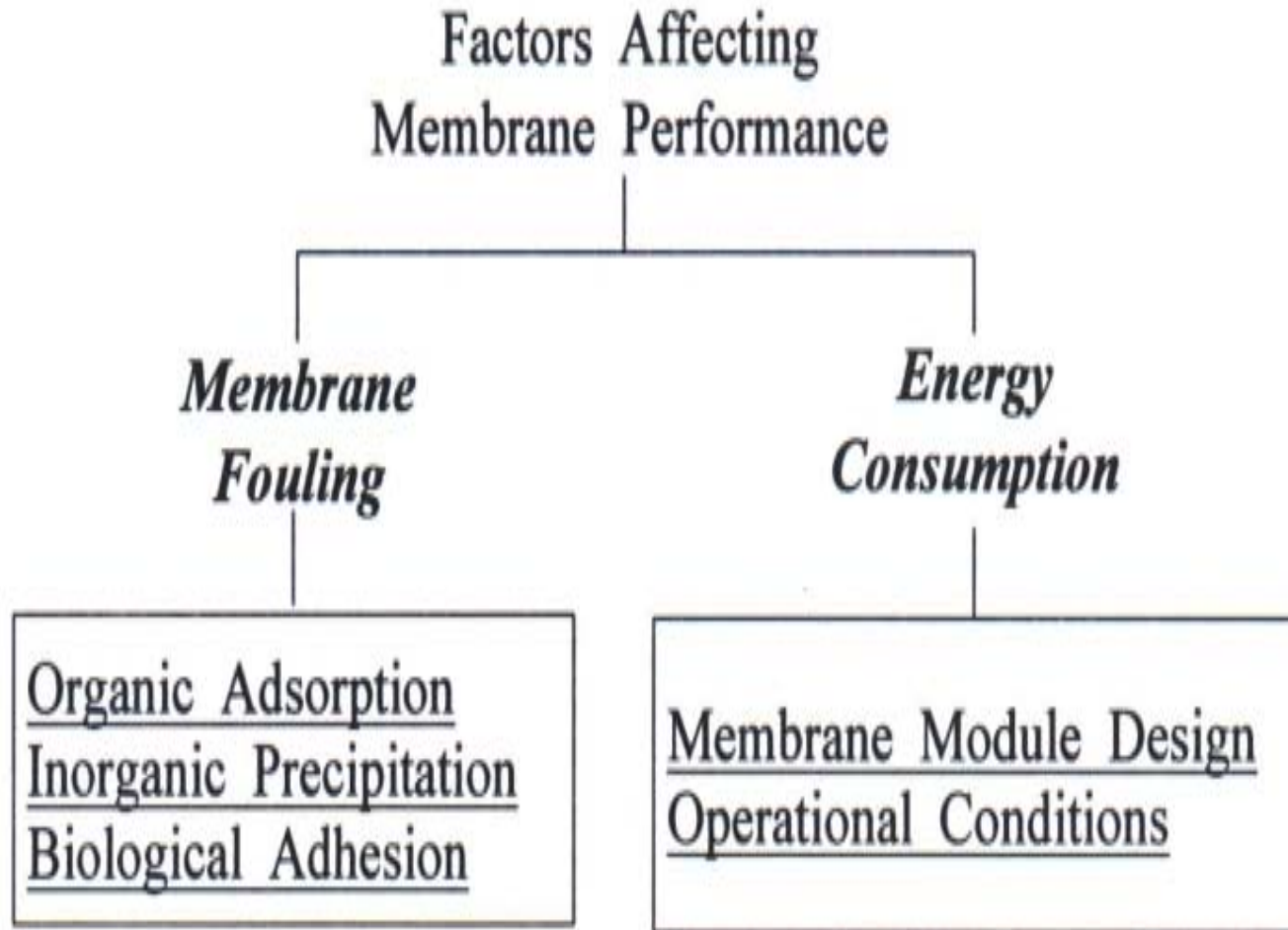


Membranes used for domestic MBR processes

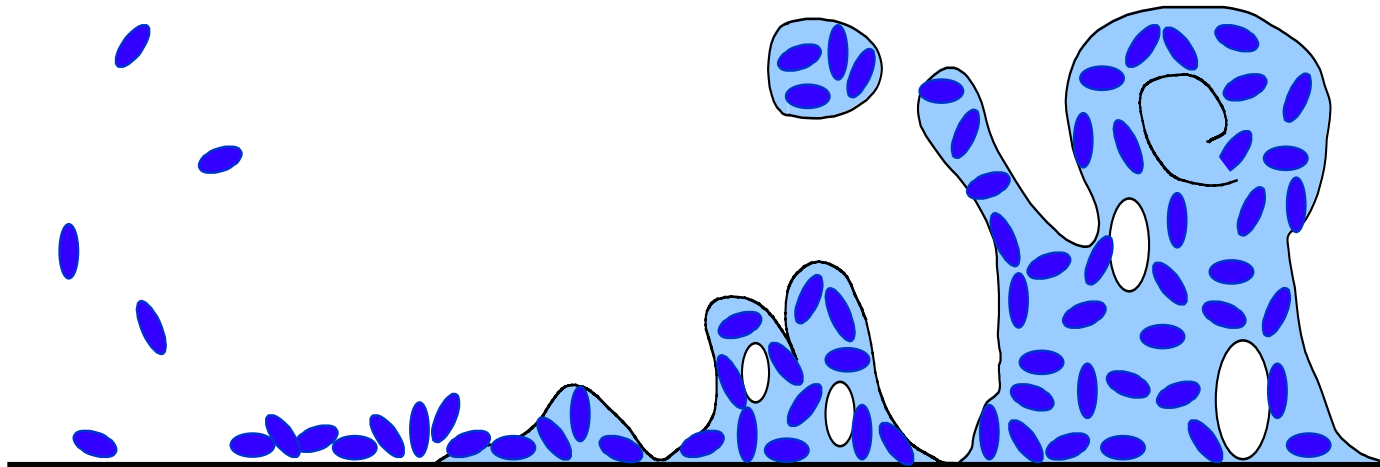
Hollow fiber	Plate	Tubular
MF	MF	UF
Out-In	Out-In	In-Out
Submerged	Crossflow/ Submerged	Crossflow



Factors Affecting Membrane Performance



Biofouling



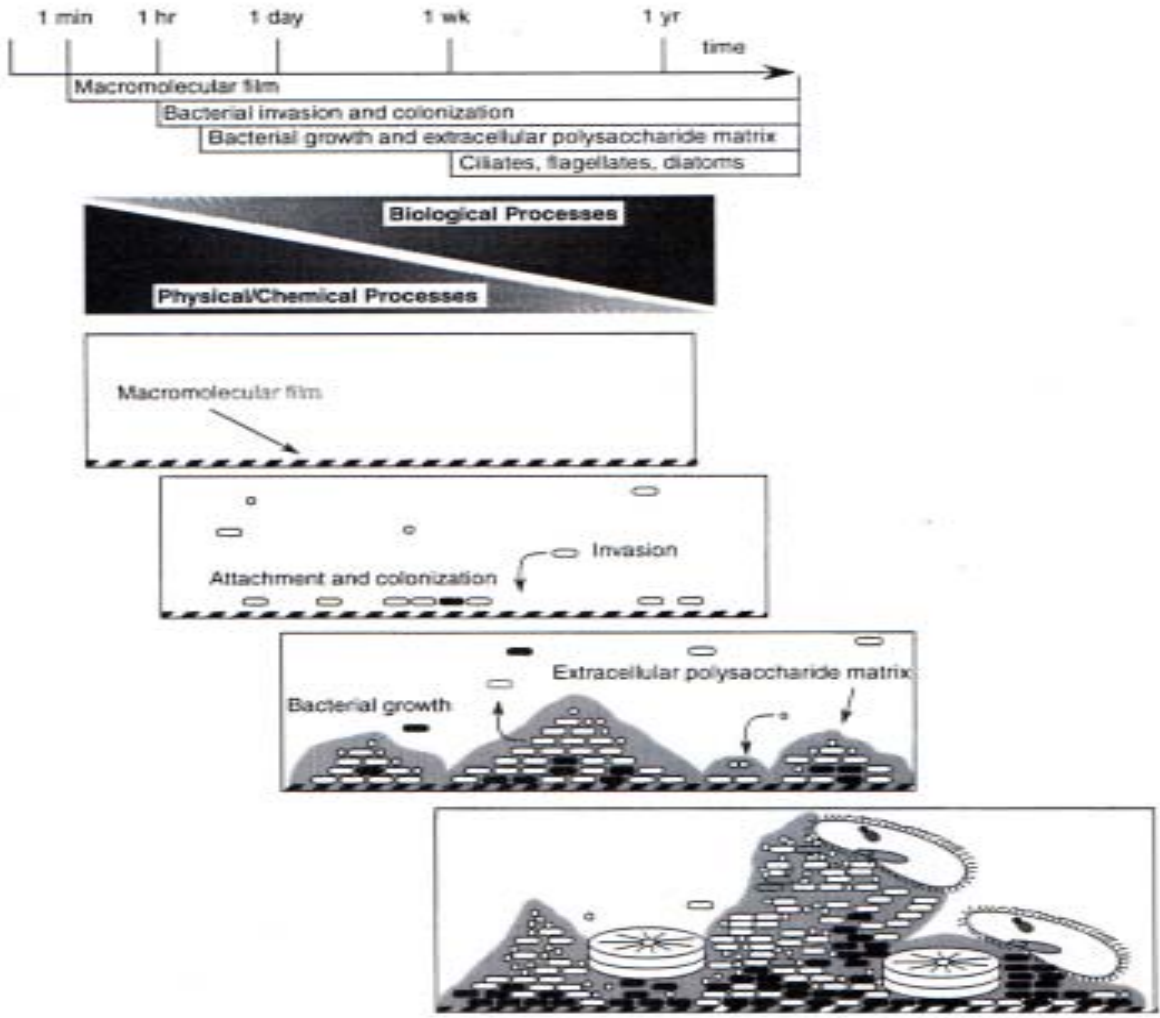
: Membranes in contact with the broth of activated sludge reactor will be colonized within short time by microorganisms, leading to the formation of a composite layer known as biofilm.

: Biofouling has restricted the widespread application of MBR, because

- i) it limits the maximum flux obtainable,**
- ii) it leads to substantial cleaning requirements,**
- iii) it shortens membrane life time**



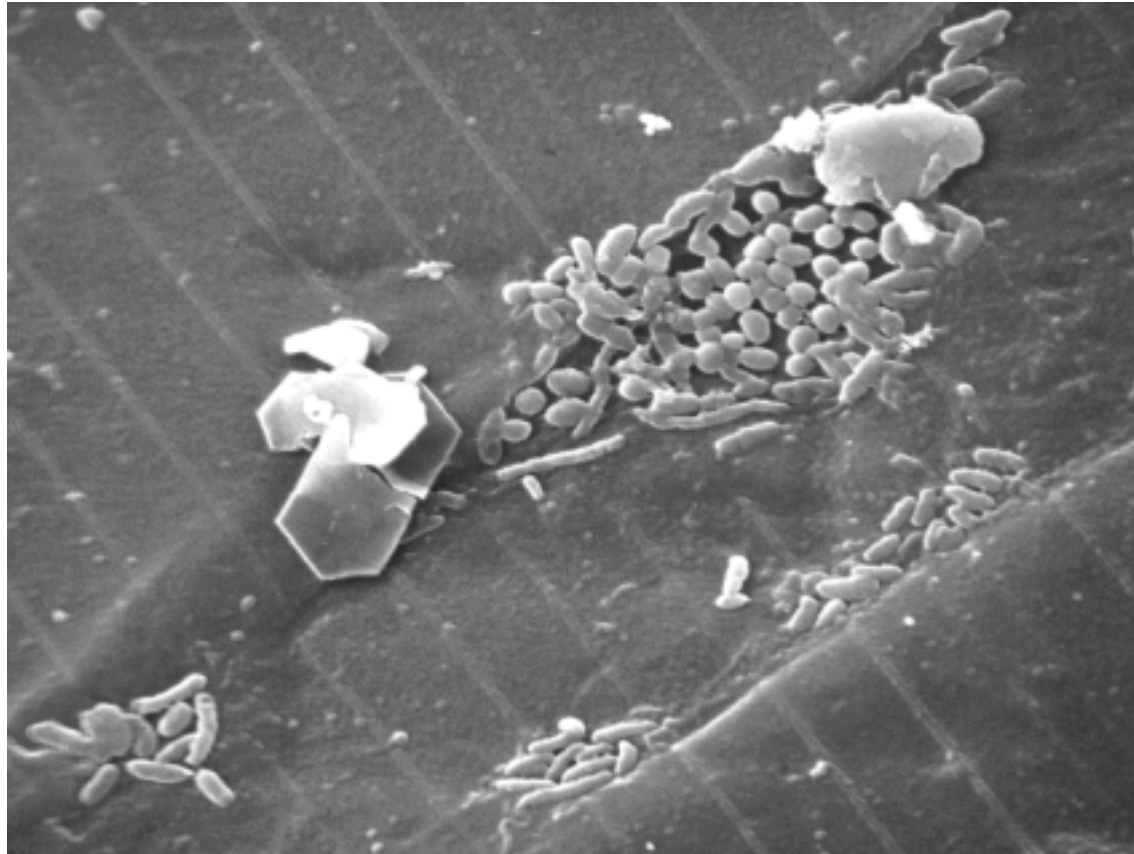
Development of Biofilm Community



Advances in Microbial Ecology, 1995

J.R. Lawrence, D.R. Korber, G.M. Wolfardt, D.E. Caldwell
Water Environment Membrane Technology Lab., Seoul National University





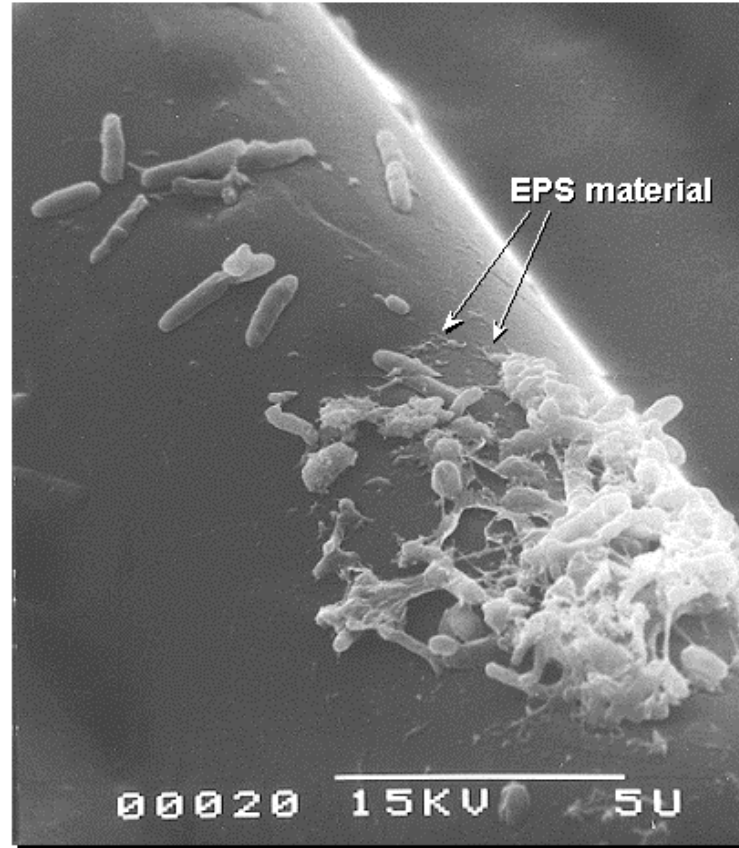
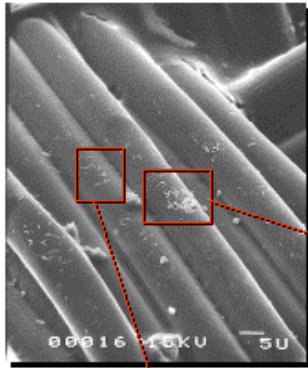
Scanning electron micrograph (SEM) of an early bacterial biofilm on the surface of a cellulose acetate (CA) reverse osmosis (RO) membrane.

In this case the RO membrane was used to demineralize pretreated municipal wastewater at Water Factory 21 in Orange County, California.

Note that the microcolonies appear to have gained foothold in low depressions (imperfections) in the membrane surface where lower hydrodynamic shear forces might be expected. Localized regions of reduced shear allows more time for bacteria to undergo irreversible attachment.



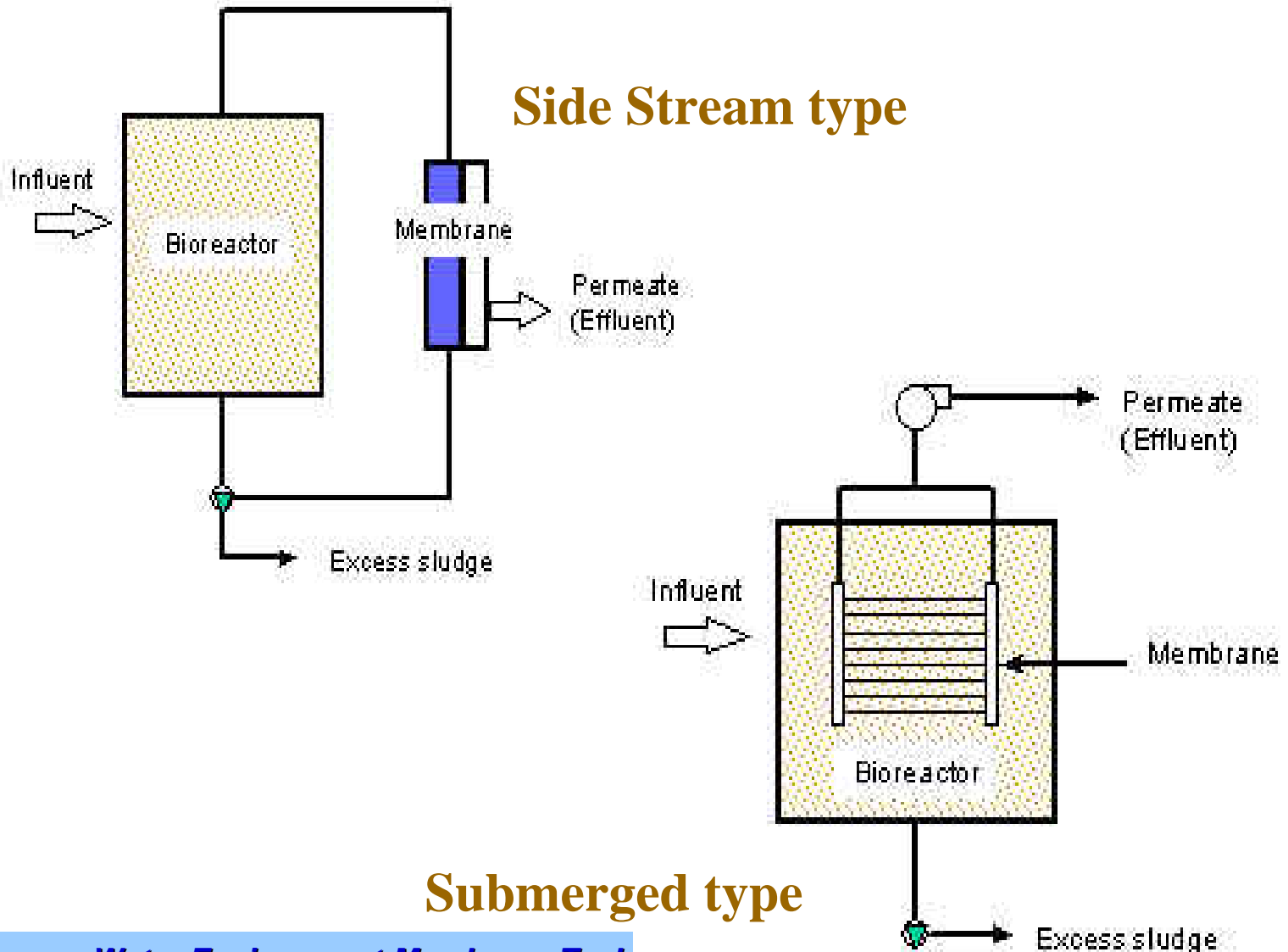
Biofouling on permeate surface of CA membrane
(Water Factory 21)

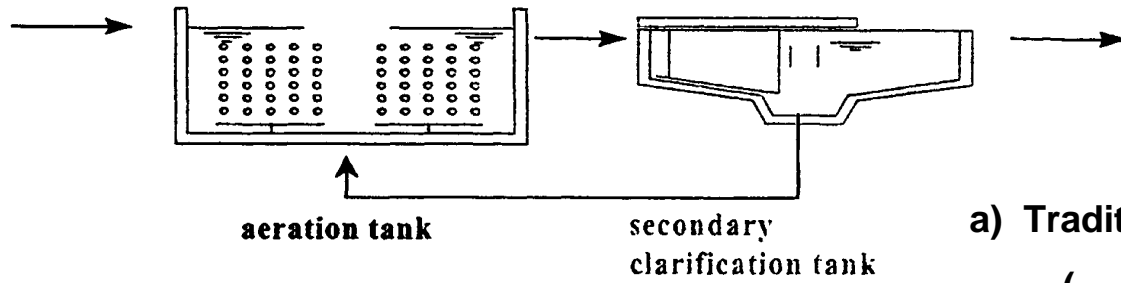


Scanning electron micrographs (SEMs) of individual cells and microcolonies growing on the permeate (product water) surfaces of polyester Texlon fibers of cellulose acetate (CA) reverse osmosis (RO) membranes. The membranes were fed with a pretreated municipal wastewater at Water Factory 21 in Orange County, California. Note the copious production of extracellular polymeric substances (EPS) by the attached bacteria, especially those cells associated with the larger microcolonies. Such EPS mediates early cell attachment and physically stabilizes and protects the biofilm.

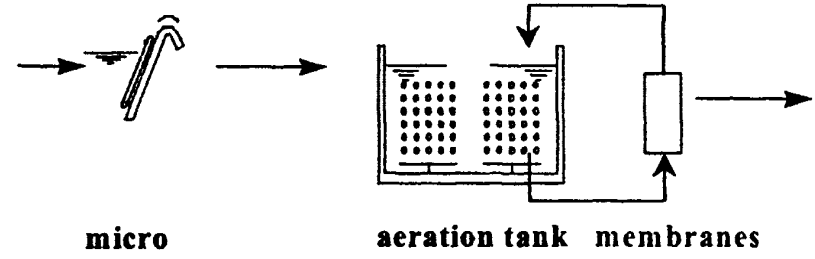


MBR for advanced wastewater

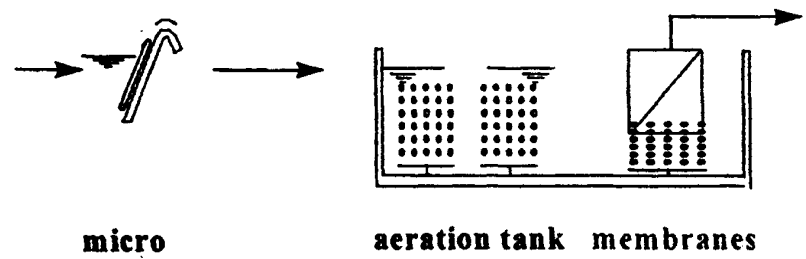




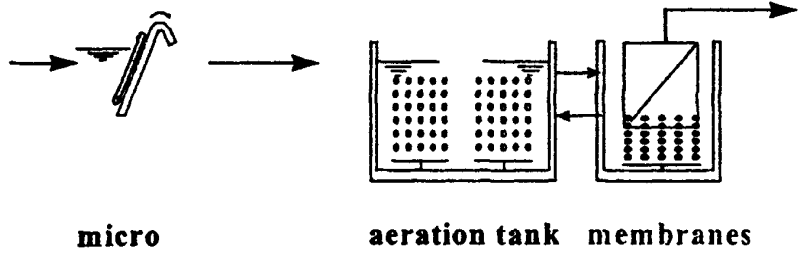
a) Traditional wastewater treatment
()



b) External crossflow and side stream
()



c) Internal submerged
()



d) External submerged
()



Models for predicting membrane performance (Flux)

1) Filtration Model

2) Resistance in Series Model

3) Film theory Model



Filtration Models

- If the solute is thought of as a 'cake' of deposited particles,
- the cake (gel, deposit, etc) resistance is obtained from filtration theory.

$$J = \frac{\Delta P}{(R_m + R_c) \cdot \eta} \quad - (1)$$

$$R_c = \alpha \cdot V C_b / A_m = \alpha \cdot m_s / A_m \quad - (2)$$

R_c : solute resistance (1/m)

R_m : membrane resistance (1/m)

V : cumulative solvent volume (m³)

C_b : bulk solute concentration (kg/m³)

A_m : membrane area (m²)

m_s : mass of solute (kg)

α : specific resistance (m/kg)



For unstirred conditions R_c grows and combining equation (1) with (2) gives,

$$J(t) = \frac{1}{A_m} \frac{dV}{dt} = \frac{\Delta P}{(R_m + \alpha \cdot VC_b / A_m) \cdot \eta} \quad - (3)$$

from eqn.(3)

$$\int_0^t dt = \int_0^V \frac{R_m \cdot \eta}{\Delta P \cdot A_m} \cdot dV + \int_0^V \frac{\alpha \cdot VC_b \cdot \eta}{\Delta P \cdot A_m^2} \cdot dV \quad - (4)$$

At constant pressure, integration of eqn.(4) gives,

$$t = \frac{R_m \cdot \eta}{\Delta P \cdot A_m} \cdot V + \frac{\alpha \cdot V^2 C_b \cdot \eta}{2\Delta P \cdot A_m^2}$$


$$\therefore t/V = \frac{R_m \cdot \eta}{\Delta P \cdot A_m} + \frac{\alpha \cdot V C_b \cdot \eta}{2\Delta P \cdot A_m^2} \quad (\text{well-known filtration equation})$$

If R_m is negligible,

$$V^2 = \frac{2 \cdot \Delta P \cdot A_m^2}{\alpha \cdot C_b \cdot \eta} \cdot t \quad - (5)$$

Which predicts that filtrate accumulates according to $t^{1/2}$



Determination of gel layer thickness

From the filtration model, it is possible to estimate the magnitude of the polarized layer (δ_s) in stirred ultrafiltration.

α : determined by unstirred experiment.

J, R_m : measurement by experiment.

From eqn. (1),(2) m_s/A_m is obtained.

ε : obtained from C_g

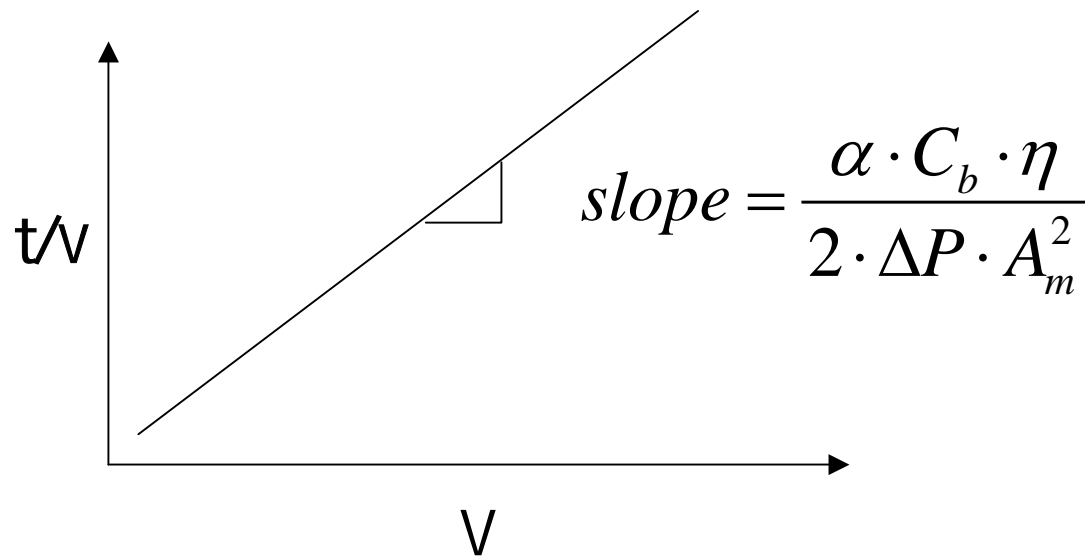
The effective thickness of the polarized solute layer (gel layer) ;

$$\delta_s = \frac{m_s}{A_m (1 - \varepsilon) \cdot \rho_s} \quad - (7)$$



Experimental determination of α

$$t/V = \frac{R_m \cdot \eta}{\Delta P \cdot A_m} + \frac{\alpha \cdot V C_b \cdot \eta}{2\Delta P \cdot A_m^2}$$



From a plot of t/v vs V , α is obtained experimentally by the slope.



Properties of α

α properties are given by the Carman-Kozeny relationship:

$$\alpha = \frac{180(1 - \varepsilon)}{\rho_s \cdot d_s^2 \cdot \varepsilon^3}$$

α : specific resistance of biofilm

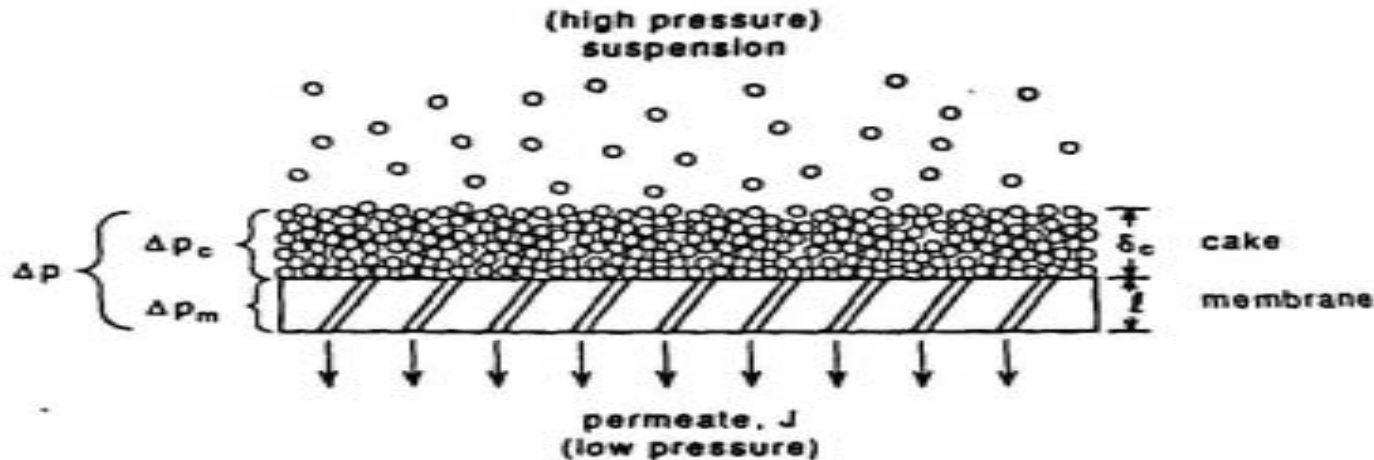
ε : Porosity

ρ : density (floc density)

d_s : size (floc diameter)



Theoretical determination of α



$$J = \frac{\Delta P}{\mu \cdot (R_m + R_C)} \quad - (1)$$

if $R_C \gg R_m$,

$$J = \frac{\Delta P}{\mu \cdot R_C} \quad - (2)$$



Theoretical determination of α

from Carman-Kozeny Equation,

$$\frac{\Delta P}{\delta_c} = \frac{K \cdot \mu \cdot (1 - \varepsilon)^2 \cdot S^2 \cdot v}{\varepsilon^3} \quad (3)$$

ΔP : pressure drop (Pa)

δ_c : thickness of cake (m)

v : superficial velocity (m/sec)

ε : porosity of filter media (dimensionless)

μ : viscosity of fluid (Pa·sec)

K : Kozeny-Carman constant ($\cong 5$)(dimensionless)

S : specific surface (area/volume) of particle (1/m)

d : particle diameter (m)



If the particle is spherical,

$$S = \frac{\pi \cdot d^2}{\pi \cdot d^3 / 6} = 6 / d \quad - (4)$$

If the particle is non-spherical,

$$S = \frac{6}{\Psi \cdot d}$$

$6/\Psi$: shape factor

$\Psi = 1$ for spherical particle.

Ψ : sphericity (dimensionless)

$$= \frac{\text{Surface area of equivalent-volume sphere}}{\text{True surface area}}$$



From eqn. (3)

$$v = \frac{\Delta P}{\delta_c} \frac{\varepsilon^3}{K \cdot \mu \cdot (1 - \varepsilon)^2 \cdot S^2}$$

$$v = \frac{\Delta P}{\delta_c} \frac{\varepsilon^3}{5\mu \cdot (1 - \varepsilon)^2 \cdot (6/d)^2}$$

$$v = \frac{\Delta P}{\delta_c} \frac{d^2 \cdot \varepsilon^3}{180\mu \cdot (1 - \varepsilon)^2} \quad \text{---(5)}$$



$$J = \frac{1}{A_m} \frac{dQ}{dt} = v$$

$$J = \frac{\Delta P}{\delta_c} \frac{d^2 \cdot \varepsilon^3}{180\mu \cdot (1 - \varepsilon)^2} \quad - \quad (6)$$

Q : volume of flow (m³/sec)

A_m : membrane area (m²)

From eq. (2) and (6)

$$R_c = \frac{180\delta_c \cdot (1 - \varepsilon)^2}{d^2 \cdot \varepsilon^3} \quad - \quad (7)$$



$$R_C = \alpha \cdot m_S / A_m - (8)$$

α : specific cake resistance (m/kg)

m_S : mass of particle deposited (kg)

ρ_S : particle density excluding water (kg/m³)

$$m_S = \delta_C \cdot A_m \cdot (1 - \varepsilon) \cdot \rho_S - (9)$$

from eqn. (7), (8) & (9)

$$\alpha = \frac{180 \cdot (1 - \varepsilon)}{\rho_S \cdot d^2 \cdot \varepsilon^3} - (10)$$



- The effect of pressure on α is frequently expressed by the relationship.

$$\alpha = \alpha_0 \cdot \Delta P^s \quad \left[\begin{array}{l} \alpha_0 : \text{constant} \\ s : \text{compressibility factor} \end{array} \right.$$

- For compressible solids, typical values of $s = 0.2 \sim 0.7$ (Fig. 2)

ΔP_g : pressure drop across the deposited solute

$$\Delta P_g = \Delta P \left(\frac{R_g}{R_m + R_g} \right) = \Delta P - R_m \cdot \eta \cdot J$$



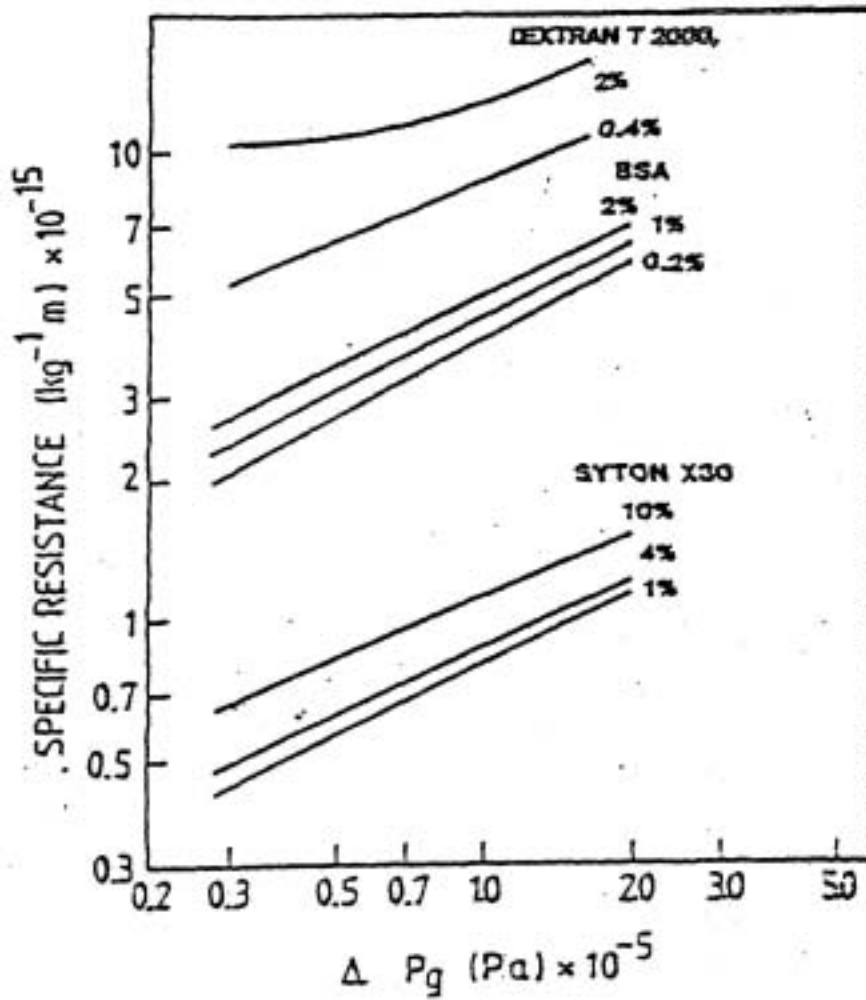


Fig. 2. Specific resistance vs Pressure



Carman-Kozeny Equation

- ◆ Hydraulic permeability(P_h)

$$P_h = \frac{d_p^2 \cdot \varepsilon^3}{180 \cdot (1 - \varepsilon)^2}$$

d_p : particle diameter (m)

ε : porosity of the cake layer (dimensionless)

- ◆ Combined with Resistance-in-series model

$$R_c \propto \frac{\mu \cdot (1 - \varepsilon)^2}{d_p^2 \cdot \varepsilon^3}$$

μ : viscosity of fluid (Pa·sec)



Models for predicting membrane performance (Flux)

1) Filtration Model

2) Resistance in Series Model

3) Film theory Model



Resistance Models

- Hagen-Poiseuille and Film Theory Model does not describe the entire pressure-flux behavior, i.e. , pressure-controlled at low pressures, pressure-independent at high pressures. Therefore ultrafiltration performance is also frequently interpreted by Resistance-in-series relationship.

1) Gel-Polarized Model.

For an ideal membrane and solute, Hagen-Poiseuille equation can be rewritten as,

$$J = \frac{\Delta P}{R_m \cdot \eta}$$

R_m : Intrinsic Membrane Resistance determined using pure water as feed.



Resistance Models

With a real feed, the membrane resistance by itself may be only a small part of the total resistance and there may be a series of additional resistances.

$$J = \frac{\Delta P}{(R'_m + R_P) \cdot \eta} = \frac{\Delta P}{(R_m + R_f + R_g + R_{BL}) \cdot \eta}$$

R_f : Fouling layer resistance (specific membrane-solute interactions, either by surface deposition or pore fouling)

R_P : Resistance attributable to the polarized solute.

R_g : Resistance due to gel-polarized layer

R_{BL} : Resistance of the viscous, but non-gelled boundary layer.



$$R_p = R_g + R_{BL}$$

$R_p = \phi \Delta P_T$ (a function of applied pressure)

- i.e. any increase in ΔP_T simply increases the thickness of the gel layer, and increase R_g .

$$\therefore J = \frac{\Delta P_T}{(R'_m + \phi \Delta P_T) \cdot \eta}$$



Remark ;

1) At High pressure, $R_p \gg R'_m$

J will become independent of ΔP_T and approach the limiting value $1/\theta$

2) At low pressure, when polarization is less ($C_w < C_g$)

$R_g=0$, \therefore J is pressure-dependent. (i.e. 'pre=gel' condition)

$$J = \frac{\Delta P_T}{(R'_m + R_{BL}) \cdot \eta}$$

3) This model suffer from having to obtain the constants experimentally.



- Unit of R_m ;

$$J = \frac{\Delta P}{R_m \cdot \eta}$$

$$\therefore R_m = \frac{\Delta P_T}{J \cdot \eta} = \frac{N / m^2}{\frac{m^3}{m^2 \cdot \text{sec}} \cdot \frac{N}{m^2} \cdot \text{sec}} = 1 / m$$

R_m is useful for modeling purpose and for evaluating the effectiveness of the cleaning procedures.



Resistance in series Models

$$J = \frac{\Delta P}{(R_m + R_f + R_c) \cdot \eta}$$

R_m : Intrinsic Membrane Resistance

R_f : Fouling layer resistance (specific membrane-solute interactions, either by surface deposition or pore fouling) ← Bulk Compositions

R_c : Cake layer resistance ← Biofilm



Models for predicting membrane performance (Flux)

1) Filtration Model

2) Resistance in Series Model

3) Film theory Model



The Film-Theory Model

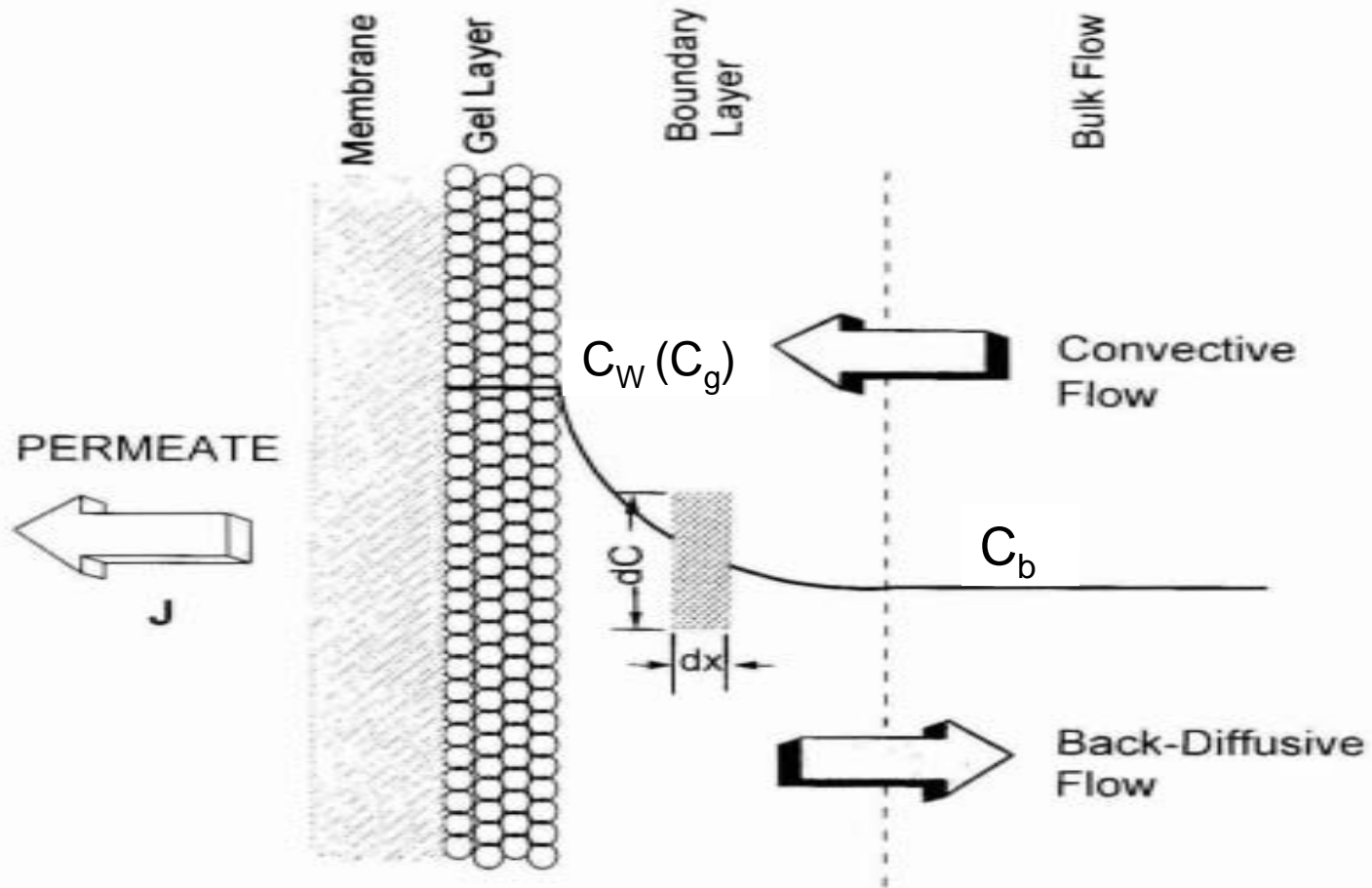


Figure 4.14. Schematic of concentration polarization during UF of colloidal and macromolecular solutes, showing the buildup of the polarized (gel) layer and associated boundary layer. The same phenomenon occurs with MF membranes, depending on the rejection of the solutes.



The Film-Theory Model

- i) Longitudinal mass transport within the boundary layer is assumed negligible (mass transfer within the film is one dimensional)
 - ii) In the steady state, the solute flux is constant throughout the film and equal to the solute flux through the membrane.
- A material balance for the solute in a different element gives the equation.

$$J_S = C_P \cdot J_V = CJ_V - D(dC / dx)$$

J_S : solute flux

J_V : solvent flux

C_b : bulk solute concentration

δ : thickness of the boundary layer

C_P : permeate solute concentration

C_w : solute concentration at the membrane surface

D : solute diffusion coefficient



Boundary Condition ; $C = \begin{cases} C_b & \text{at } x=0 \\ C_w & \text{at } x= \delta \end{cases}$

$$D \cdot \frac{dC}{dx} = J_V (C - C_P)$$

$$\int_{C_b}^{C_w} D \cdot \frac{dC}{C - C_P} = \int_0^{\delta} J_V \cdot dx \rightarrow D \cdot \ln(C - C_P) \Big|_{C_b}^{C_w} = J_V \cdot \delta$$

$$\therefore J_V = \frac{D}{\delta} \ln \left(\frac{C_w - C_P}{C_b - C_P} \right) = k_S \cdot \ln \left(\frac{C_w - C_P}{C_b - C_P} \right)$$

$$J_V = k_S \cdot \ln \frac{C_w}{C_b} \quad (\text{if } C_P = 0)$$

$$D/\delta = k_S$$

k_S : mass-transfer coefficient



- If $C_w \rightarrow C_g$

$$J_{\text{lim}} = k_s \cdot \ln \frac{C_g}{C_b} \quad (\text{Gel polarization Model})$$

C_g : Gel Concentration

J_{lim} : limiting flux

- Observed retention ; $S=1-C_p/C_b$, True retention ; $R=1-C_p/C_w$
The concentration polarization ; $M=C_w/C_b = 1-S+S \exp(J_v/k_s)$
So, M can be calculated from the measurement of the retention and the permeate flux, when k_s is known.



Remark;

- 1) This model will be valid only in the pressure-independent region.
(there is no pressure term) (Fig. 4.13)
- 2) Flux will be controlled by the rate at which solute is transferred back from the membrane surface into the bulk fluid.
- 3) Flux can only be improved by enhancing k_s as much as possible, such as by reducing the thickness of the boundary layer (δ)
- 4) C_g is fixed by physicochemical properties of the feed.

L_m : permeability coefficient



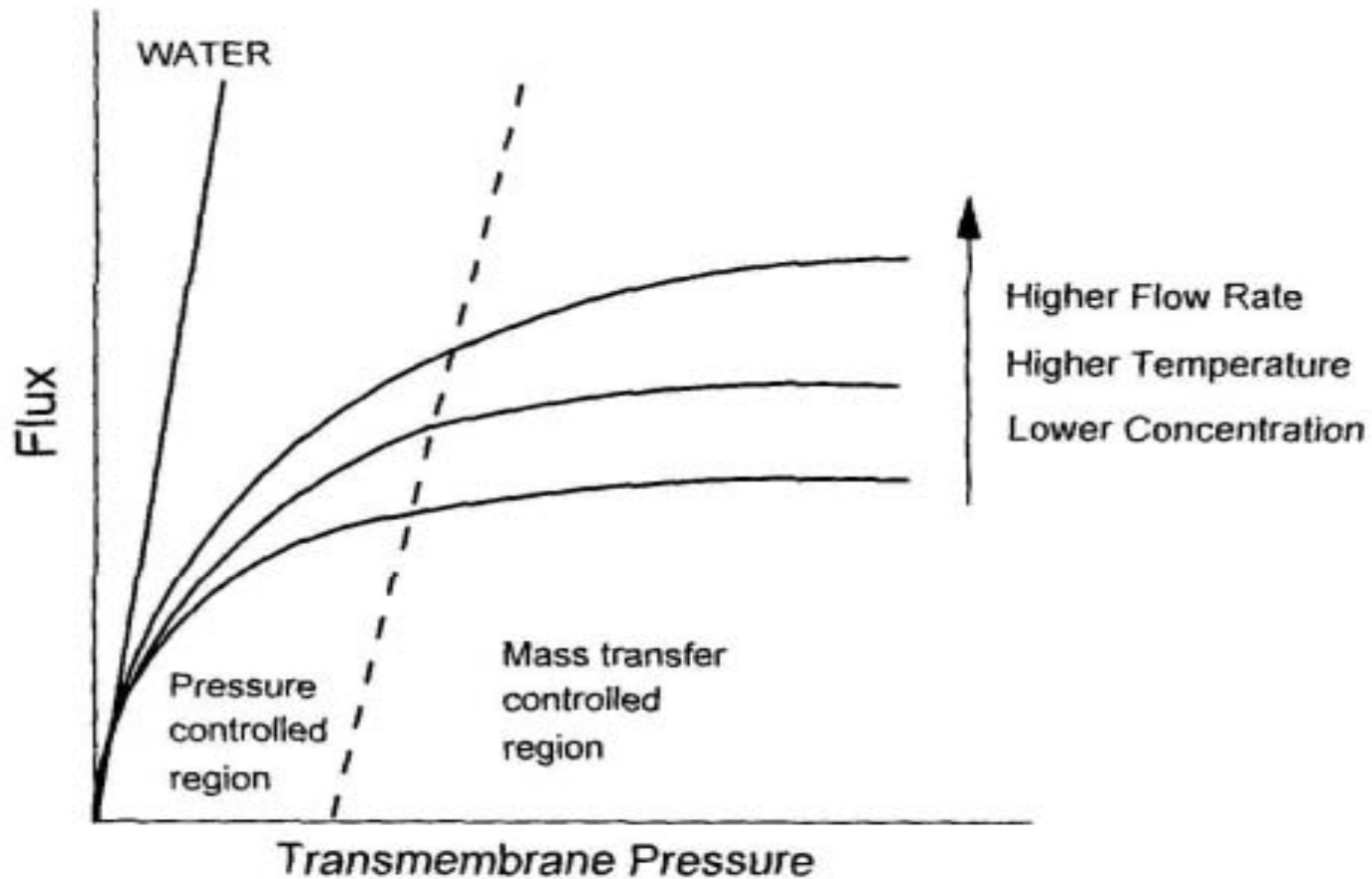


Figure 4.13. Generalized correlation between operating parameters and flux, indicating the areas of pressure control and mass transfer control.

Remark;

5) J_{lim} should be independent of membrane properties.

It is determined by C_g , C_b and k_s (hydrodynamic conditions)

(But Fane showed that 'gel-polarized' behavior with identical solutions and hydrodynamics produced different J_{lim} values when membranes of differing permeability, L_m)

6) Feed solutions of various macrosolutes with concentration did not give zero flux.

7) If C_g is a 'gel' concentration, it should depend only on the nature of the solute, but it appears to vary with system-hydrodynamics.

8) This model appears to have physical limitations although it still remains the most convenient model from a practical point of view.

L_m : permeability coefficient



Flux Paradox

Film theory model – for macromolecule solutions

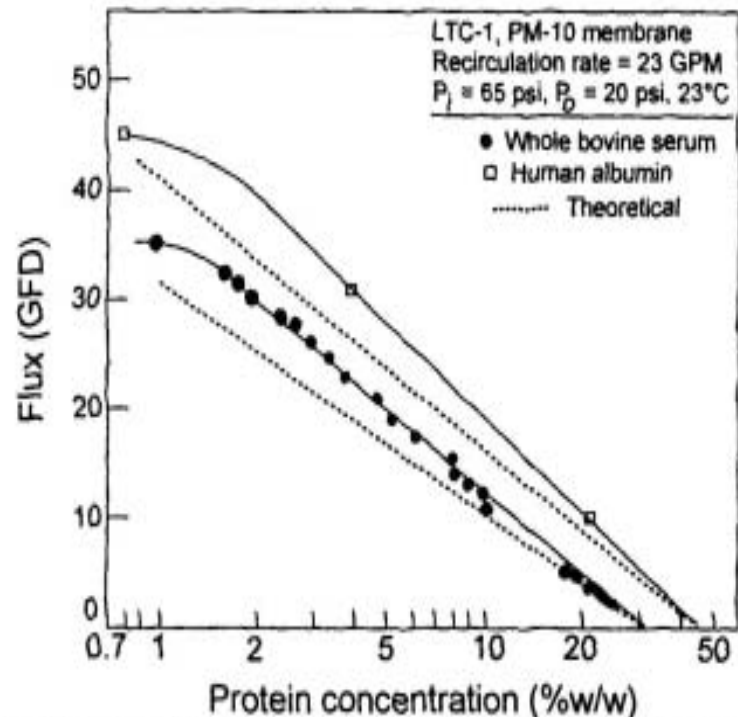


Figure 4.18. Relationship between flux and protein concentration during concentration of human albumin and whole bovine serum. The module was a 15-mil thin-channel laminar flow unit with Amicon PM-10 membrane. Theoretical lines were drawn using the Leveque solution and the film theory, with diffusion coefficients of 4×10^{-7} cm²/sec for whole bovine serum and 6×10^{-7} cm²/sec for human albumin (adapted from Porter, 1979).



Film theory model – for colloidal suspensions

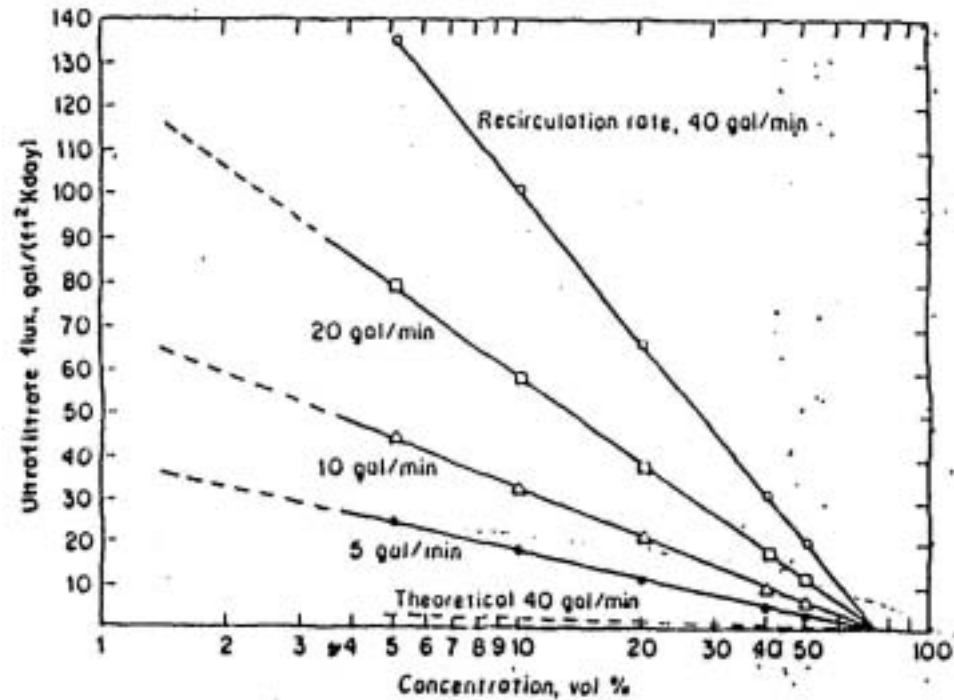


Figure 4.21. Ultrafiltration of styrene-butadiene polymer latex in LTC-1, 15-mil channel, XM-50 membrane, 60 psig pressure (From Porter, 1979).



Flux Paradox

- 1) For macromolecular solutions, the agreement between theoretical and experimental ultrafiltration rates is within 15~30%.
- 2) For colloidal suspensions, experimental flux values are often one to two orders of magnitude higher than those indicated by the L ev eque and Dittus-Boelter relationships. But the reason is not clear.
- 3) In colloidal suspensions, the diffusion coefficient calculated from the ultrafiltrate flux using the L ev eque and Dittus-Boelter equations is generally from one to three orders of magnitude higher than the theoretical Stokes-Einstein diffusivity.
- 4) Minor adjustments in molecular parameters such as diffusivity (D), kinematic viscosity (ν), or gel concentration (C_g) are incapable of resolving order of magnitude discrepancies.



5) Back-diffusive transport of colloidal particles away from the membrane surface into the bulk stream ($D \cdot \partial C / \partial x$) is substantially augmented over that predicted by the L ev eque and Dittus-Boelter relationships.

6) For colloidal suspensions, mass transfer from the membrane into the bulk stream is driven by some force other than the “concentration gradient”.

M.C. Porter’s opinion (1972) : Tubular Pinch Effect is responsible for this augmented mass transfer.



Tubular Pinch Effect

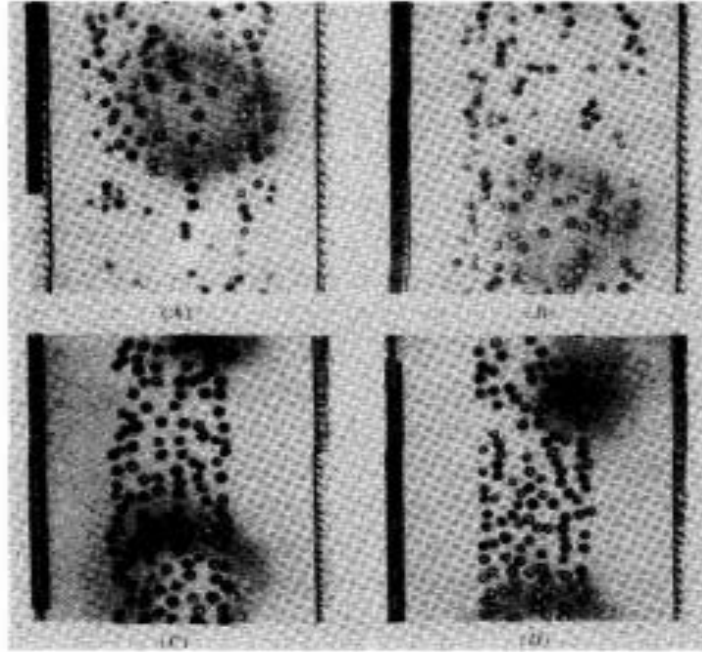


Figure 4.34. The tubular pinch effect. Particles of 1-mm diameter were flowing in a 15% aqueous glycerin solution. Particle concentration = 5%, channel $Re = 900$, particle $Re = 225$ (adapted from Brandt and Bugliarello 1966).

- Segré and Silberberg : the first to publish the observations of the tubular pinch effect. (As the particles were flowing through a tube, the particles migrated away both from the tube wall and the tube axis, reaching equilibrium at an eccentric radial position.)



Forces acting on a suspended particle

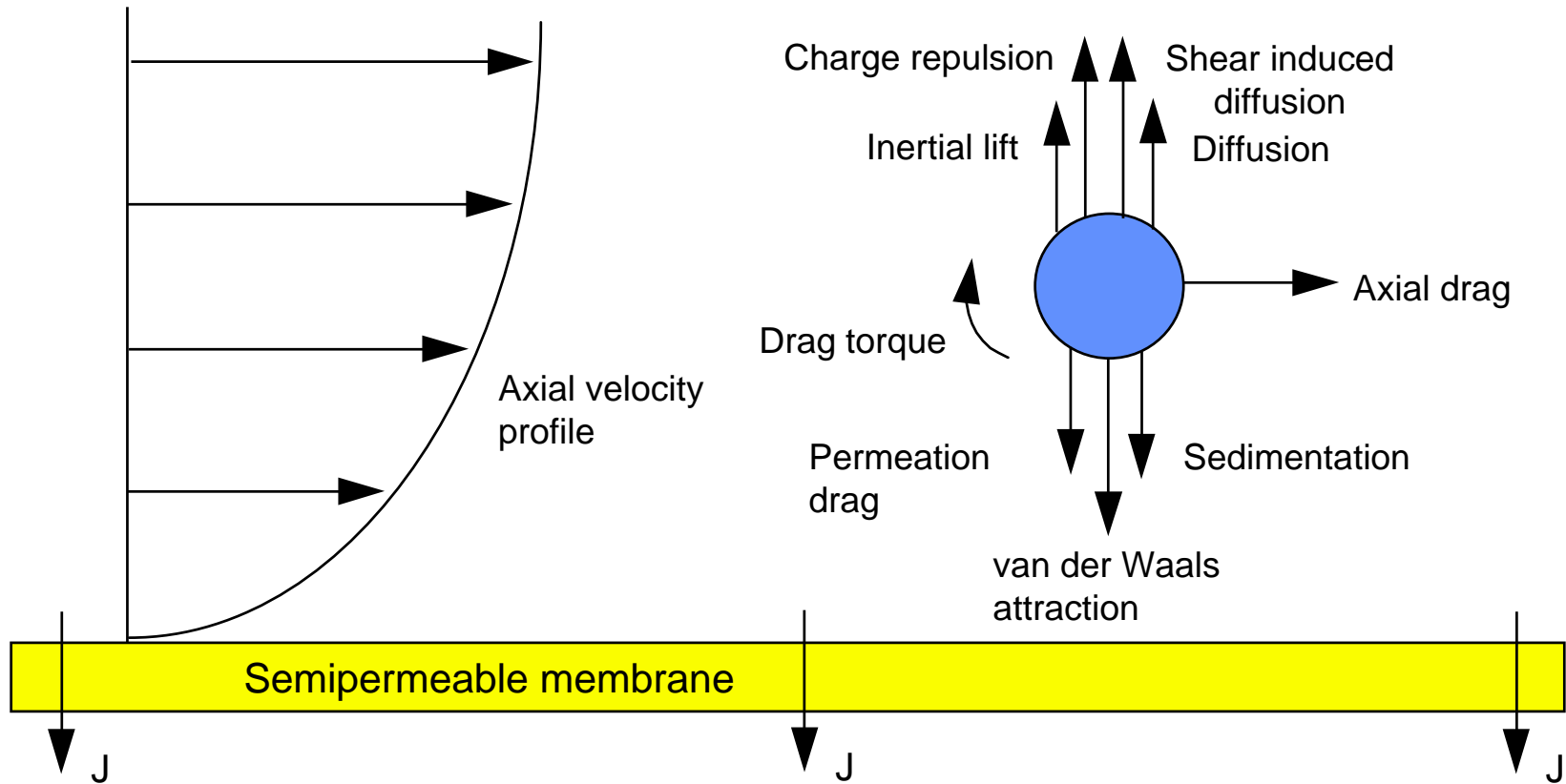


Fig. -1. Forces and torques acting on a charged, spherical particle suspended in a viscous fluid undergoing laminar flow in the proximity of a flat porous surface.[modified from Wiesner(1992)]

Table 1. Factors Affecting Particle Transport in Crossflow Membrane Filtration *

Factor	Expression †
<i>Toward the membrane</i>	
Gravity	$v_g = \frac{\pi}{18\eta} d_p^2 \rho_p g$
Van der Waals attraction	$v_A = \frac{A}{36\pi\eta s^2}$
Permeation drag (flux)	J
<i>Away from the membrane</i>	
Buoyancy	$v_b = \frac{\pi}{18\eta} d_p^2 \rho_l g$
Electrical double layer repulsion	$v_k = \frac{2\kappa\epsilon\zeta^2 \exp(-\kappa s)}{3\eta}$
Brownian diffusion	$v_B = \frac{kT}{3\pi\eta d_p \delta}$
Shear-induced diffusion	$v_s = 0.0225 \frac{u_a d_p^2}{h\delta}$
Lateral migration	$v_l = \frac{13.8}{128} \frac{\rho_p u_a^2 d_p^3}{\eta h^2}$

* Membrane module: plate and frame.

† d_p , particle diameter; ρ_p , particle density; η , dynamic viscosity; A , Hamaker constant; s , separation distance; ρ_l , liquid viscosity; κ , Debye-Hückel parameter; ϵ , fluid permittivity; δ , boundary layer thickness calculated by the L ev eque equation; ζ , zeta potential; u_a , average fluid velocity; h , half-channel height.



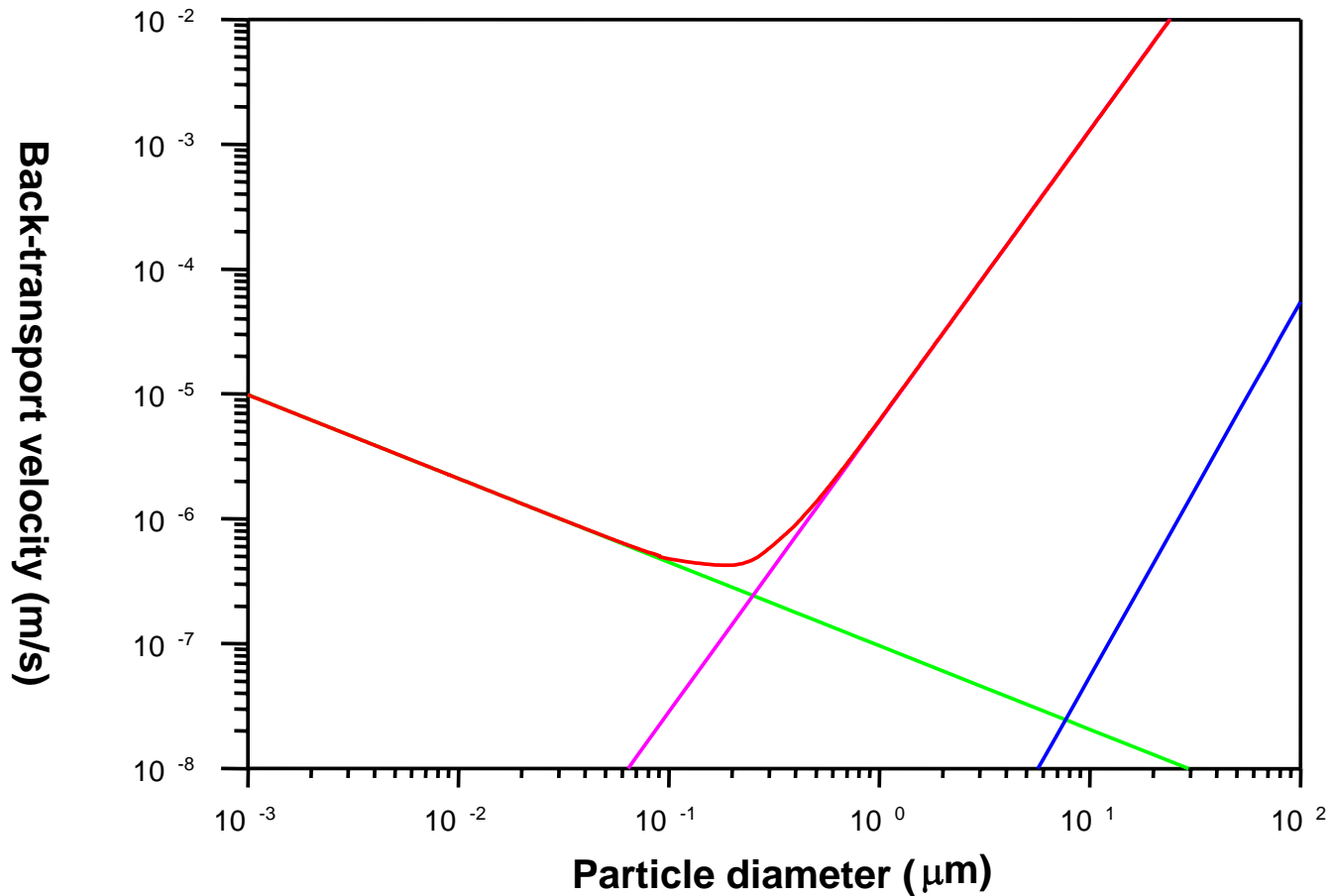


Fig. 7.7. Back-transport velocity based on different migration mechanisms.



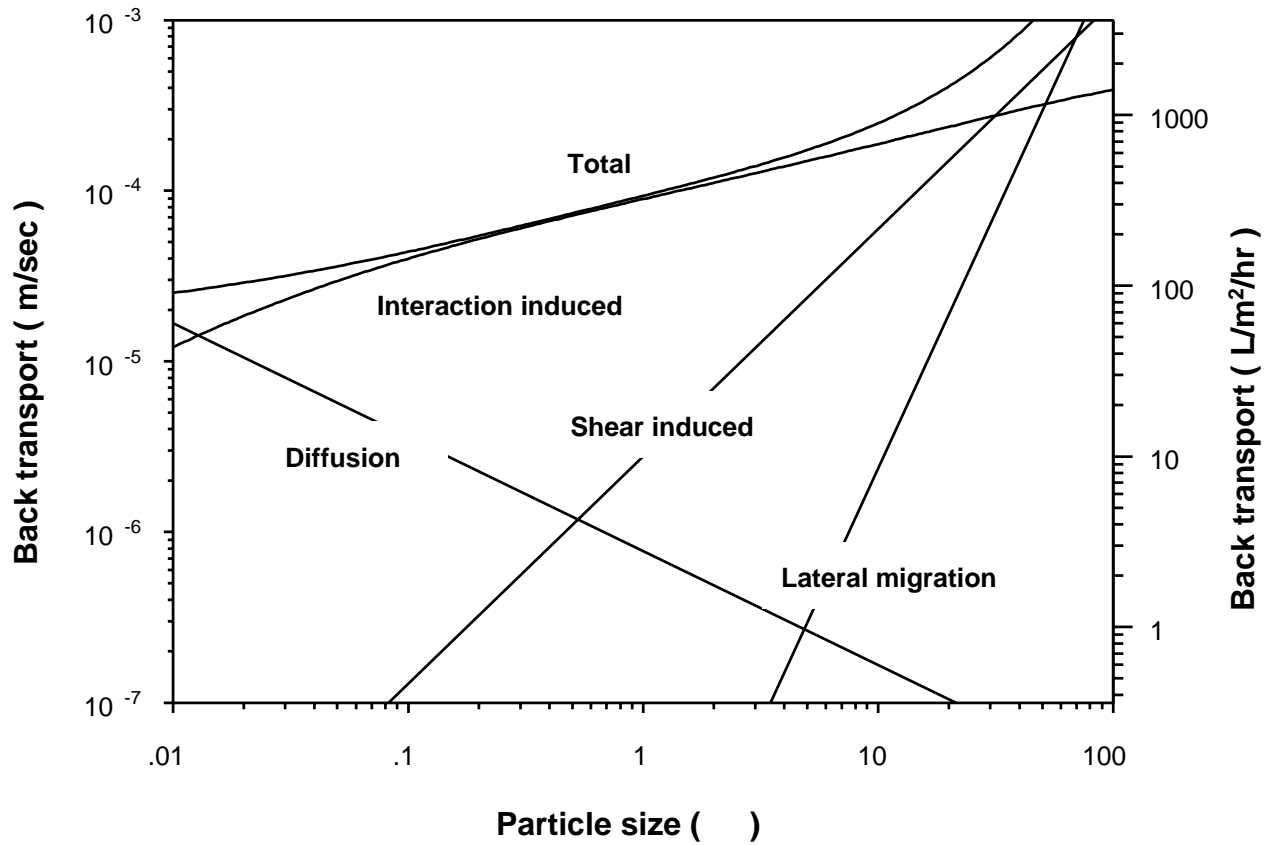


Fig. -4. Comparison of different models explaining a critical flux over a range of particle size.



Remark :

- 1) Crossflow microfilters are occasionally operated in the turbulent regime, whereas all of the models described are restricted to laminar flow.
- 2) Brownian and shear-induced diffusion may be considered simultaneously by adding the diffusion coefficients, although recent simulations have shown that the diffusion coefficients are not strictly additive.
- 3) The models described are based on idealized suspensions of equi-sized spheres, which do not irreversibly stick to the membrane or cake surfaces but rather are free to diffuse or lift away. Further experiments and models are needed to study Brownian, shear induced diffusion, and inertial lift in real suspensions of non-spherical, deformable particles having both narrow and broad size distributions.



4) Considerable experimental and theoretical research remains to complete our understanding of crossflow microfiltration.

For example, issue of direct membrane fouling by the attachment of particles and precipitates to the membrane pores and surface have not been adequately addressed.



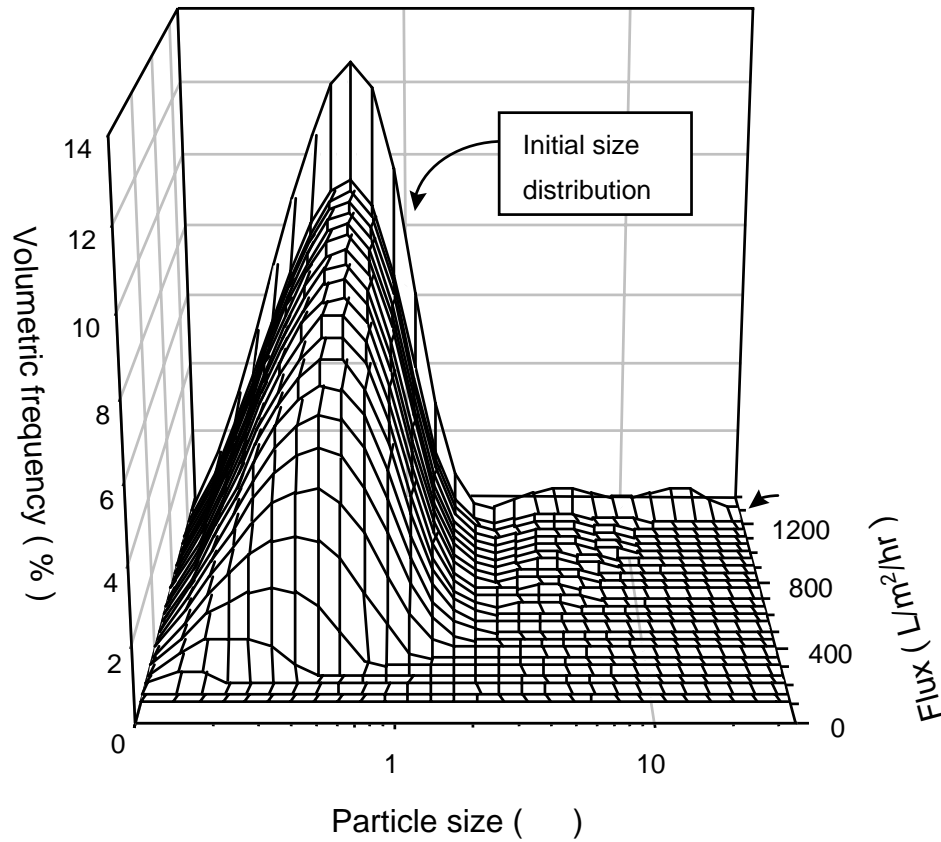


Fig. -5. Depositing particle size distribution for each flux condition. Size distribution when flux is infinite means the initial particle size distribution measured experimentally ($T = 298 \text{ K}$, $\Psi_0 = 50 \text{ mV}$, $A = 3.4 \times 10^{-20} \text{ J}$).



Membrane Fouling: Identification and Prevention

Membrane fouling

Physiochemical Approach

- ✓ Process Design
- ✓ Chemical additives
- ✓ Membrane surface modification
- ✓ Hybrid system

Microbiological Approach

- ✓ Quorum sensing mechanism
- ✓ Biofouling mechanism
- ✓ Cell physiology
- ✓ Micro-organism population dynamics

Hydrodynamic Approach

- ✓ Back transport velocity
- ✓ Critical flux



Membrane Fouling: Identification and Prevention

Physicochemical Approach:

Examples for submerged MBR systems:

- reduce flux (J)
- increase membrane aeration
- employ physical or chemical cleaning
 - backflushing (HF only)
 - relaxation (ceasing permeation whilst continuing aeration)
 - in-situ clean (*chemically enhanced backwash*)
 - ex-situ clean (*soak*)
- *all have cost implications*



Membrane Fouling: Identification and Prevention

Microbiological Approach

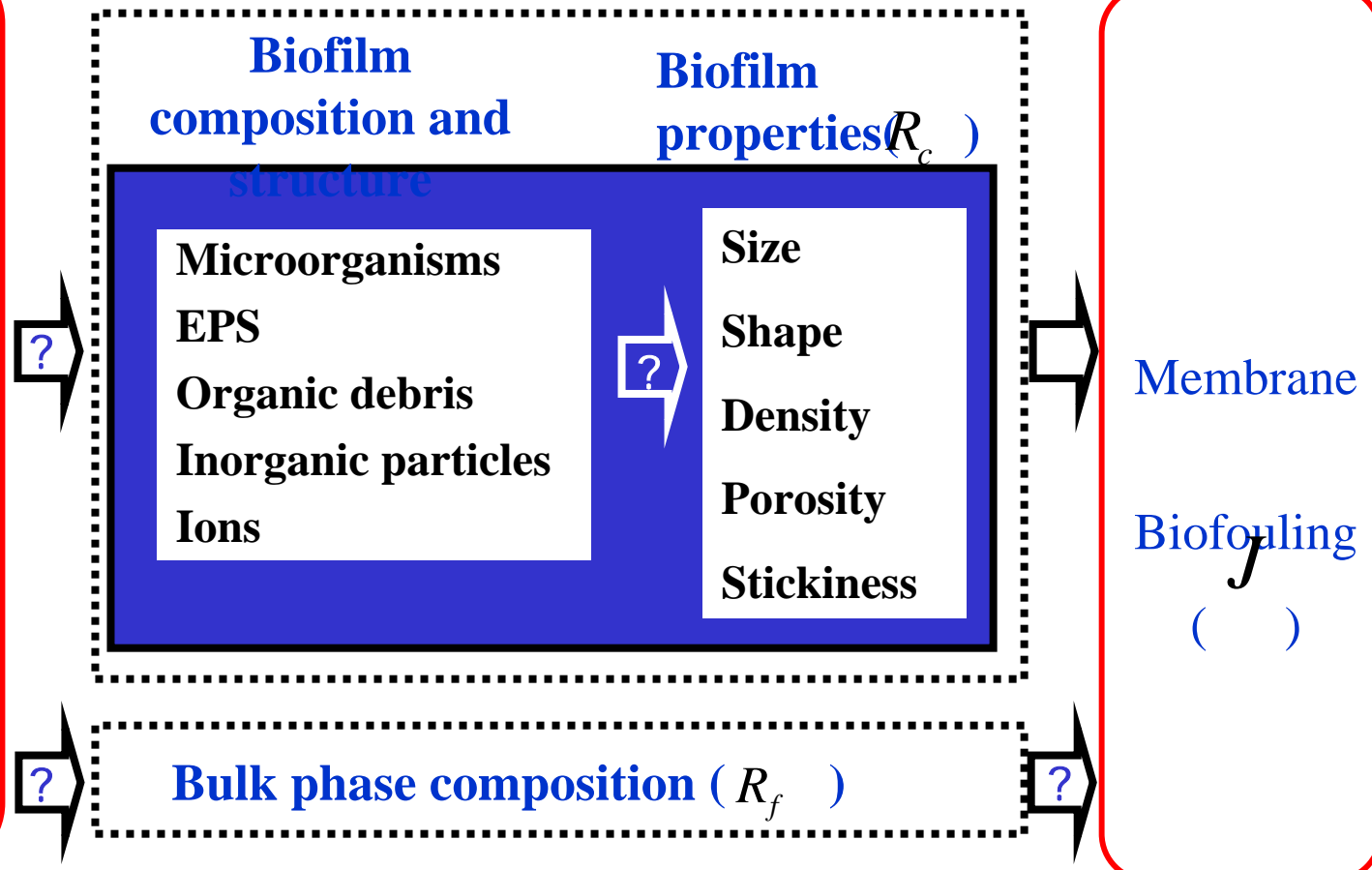
- Change of microbial characteristics :
 - Floc morphology & size,
 - Physiological state,
 - EPSs(extracellular polymeric substances) content



Overview of factors leading to membrane biofouling

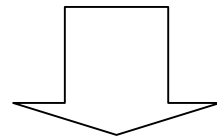
Environmental Factors in MBR

- Substrates
- DO
- Air flow rate & bubble size
- pH
- Temperature
- Growth mode (attached or suspended)
- Growth phase (log or endogenous)
- Cyclic format in SBR
- etc



Research on MBR in 21C

- ❑ Quorum sensing mechanism
- ❑ Biofilm formation mechanism
- ❑ Cell Morphology & Physiology
- ❑ Microorganism population dynamics



Innovative MBR process

